

Study of Hadronic B and B_s^0 Decays at Belle

Shawn Dubey for the Belle Collaboration^{a,*}

^a*Department of Physics and Astronomy,
University of Hawaii at Manoa,
2505 Correa Road, Honolulu, Hawaii
United States of America*

E-mail: sdubey@hawaii.edu

...

*** *The European Physical Society Conference on High Energy Physics (EPS-HEP2021), ****

*** *26-30 July 2021 ****

*** *Online conference, jointly organized by Universität Hamburg and the research center DESY ****

*Speaker

1. Motivation

The study of hadronic B and B_s^0 decays provides opportunities to search for new physics beyond the Standard Model (SM). The decays of the B and B_s^0 mesons that will be discussed here are suppressed in the SM and may be sensitive to new physics such as non-standard flavor-changing neutral currents (FCNCs). Discussed here are four different decay modes: $B_s^0 \rightarrow \eta'(\rightarrow \eta\pi^+\pi^-)X_{s\bar{s}}$, $B_s^0 \rightarrow \eta\eta'(\rightarrow \eta\pi^+\pi^-)$, $B_s^0 \rightarrow D_s^- X$, and $B^+ \rightarrow K^+ K^- \pi^-$. Charge conjugation is implied throughout unless otherwise stated specifically.

The Belle experiment provides unique possibilities for studying these decays, utilizing its large data samples. Belle collected 711 fb^{-1} at the $\Upsilon(4S)$ resonance and 121.4 fb^{-1} at the $\Upsilon(5S)$ resonance.

The $\Upsilon(5S)$ decays in three ways to B_s^0 : $\Upsilon(5S) \rightarrow B_s^{0*} \bar{B}_s^{0*}$, $B_s^{0*} \bar{B}_s^0 / B_s^0 \bar{B}_s^{0*}$, and $B_s^0 \bar{B}_s^0$, with fractions 0.87, 0.073, and 0.057, respectively [1].

2. $B_s^0 \rightarrow \eta' X_{s\bar{s}}$

Belle's search for $B_s^0 \rightarrow \eta'(\rightarrow \eta\pi^+\pi^-)X_{s\bar{s}}$ is the world's first. Here we use a semi-inclusive method whereby the $X_{s\bar{s}}$ system is reconstructed as a system of two kaons and up to four pions, with at most one π^0 . The signal is divided into two classes that can contain either zero or one K^0 that is only reconstructed as a K_S^0 , i.e. $B_s^0 \rightarrow \eta' K^+ K^- + n\pi$ and $B_s^0 \rightarrow \eta' K^\pm K_S^0 + n\pi$. The soft photon from $B_s^{0*} \rightarrow B_s^0 \gamma$ is not reconstructed.

After all final selections are applied, the signal yield is extracted using 1-dimensional unbinned maximum likelihood fits in the beam-energy-constrained mass, M_{bc} , in $200 \text{ MeV}/c^2$ bins of $X_{s\bar{s}}$ mass, in the range $M(X_{s\bar{s}}) \in [0.8, 2.4] \text{ GeV}/c^2$. The beam-energy-constrained mass is $\sqrt{E_{\text{beam}}^2/c^4 - p_{B_s}^2/c^2}$, where p_{B_s} is the magnitude of the B_s^0 three-momentum in the center-of-mass frame of the colliding e^+e^- beams, and $E_{\text{beam}} = \sqrt{s}/2$.

Fitting the M_{bc} distributions in bins of $X_{s\bar{s}}$ mass is performed separately for the two classes of signatures (with and without K_S^0). Fit results are used to determine a branching fraction (BF) central value in each $X_{s\bar{s}}$ mass bin. Within a signal class these central values are summed. A weighted average of the resulting sums of each of the classes is then obtained. The sums of the fit results overlaid on the data are shown in Fig. 1.

No statistically significant signal is found and the final central value for the BF is determined to be $\mathcal{B}(B_s^0 \rightarrow \eta' X_{s\bar{s}}) = [-0.7 \pm 8.1 \text{ (stat.)} \pm 0.7 \text{ (syst.)} \pm_{-6.0}^{+3.0} \text{ (FM)} \pm 0.1 \text{ (} N_{B_s^{0(*)} \bar{B}_s^{0(*)}} \text{)}] \times 10^{-4}$ for $M(X_{s\bar{s}}) \leq 2.4 \text{ GeV}/c^2$, which includes B_s^0 and \bar{B}_s^0 . Further, assuming $SU(3)$ symmetry, the ratio of the BFs for $B \rightarrow \eta' X_s$ and $B_s^0 \rightarrow \eta' X_{s\bar{s}}$, $\mathcal{R}(\eta')$, would be approximately 1 [3]. The BABAR collaboration measured $\mathcal{B}(B \rightarrow \eta' X_s) = [3.9 \pm 0.8 \text{ (stat.)} \pm 0.5 \text{ (syst.)} \pm 0.8 \text{ (model)}] \times 10^{-4}$, for the same $M(X_s)$ range [4]. Using these results we obtain $\mathcal{R}(\eta') = -0.2 \pm 2.1 \text{ (stat.)} \pm 0.2 \text{ (syst.)} \pm_{-1.5}^{+0.8} \text{ (FM)} \pm 0.03 \text{ (} N_{B_s^{0(*)} \bar{B}_s^{0(*)}} \text{)}$. The uncertainty due to the fragmentation model (FM) of the $X_{s\bar{s}}$ in PYTHIA 6 [5] is the largest systematic uncertainty.

The final 90% confidence level upper limits are $\mathcal{B}(B_s^0 \rightarrow \eta' X_{s\bar{s}}) < 1.4 \times 10^{-3}$ and $\mathcal{R}(\eta') < 3.5$ [2].

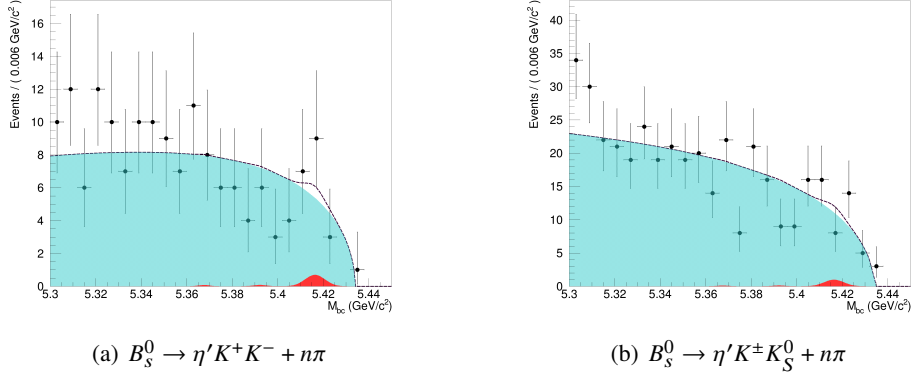


Figure 1: Sum of the fits for $M(X_{s\bar{s}}) \in [0.8, 2.4] \text{ GeV}/c^2$ (black dashed line) overlaid on the data (black points with error bars), for the two signal classes. The red-orange shade is the signal (for which there are three peaks, corresponding to the three $\Upsilon(5S)$ decay channels; the largest peak corresponds to the $\Upsilon(5S) \rightarrow B_s^{0*} \bar{B}_s^{0*}$ channel) and the light blue shade is the non-peaking background contribution [2].

3. $B_s^0 \rightarrow \eta\eta'$

The decay $B_s^0 \rightarrow \eta\eta'$ is suppressed in the SM and is sensitive to new physics such as fourth generation fermions, a two-Higgs doublet with a FCNC, etc.

After the final selections are applied, the signal extraction is performed using a 3-dimensional unbinned maximum likelihood fit in $M_{bc} - \Delta E - M(\eta\pi^+\pi^-)$. Here ΔE is defined as $\Delta E = E_{B_s} - E_{\text{beam}}$.

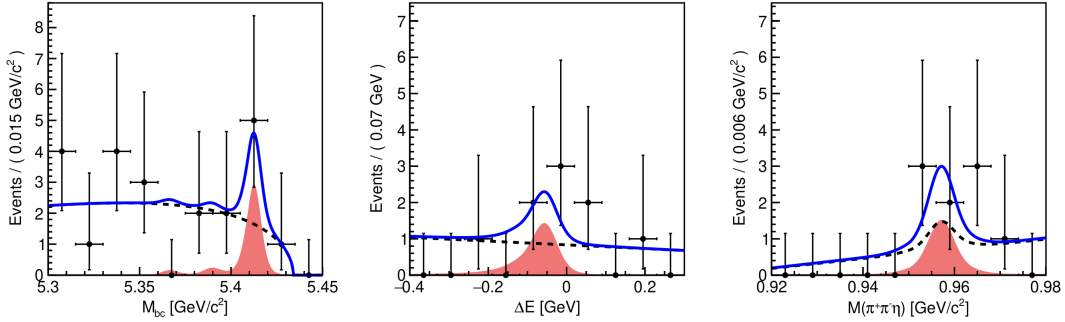


Figure 2: Fit projections in the signal region. Black points with error bars are the data, the pink shaded region is the signal component, the black dashed line is the background component, and the blue solid line is the fit result. For the ΔE and $M(\eta\pi^+\pi^-)$ fit projection plots, $5.39 < M_{bc} < 5.43 \text{ GeV}/c^2$ is required [6].

The projections of this fit onto the individual variables are shown in Fig. 2. From this fit we find 2.7 ± 2.5 signal events and 57.3 ± 7.8 background events. The resulting BF is $\mathcal{B}(B_s^0 \rightarrow \eta\eta') = [2.5 \pm 2.2 \text{ (stat.)} \pm 0.6 \text{ (syst.)}] \times 10^{-5}$. As this is not statistically significant we place a 90% confidence level upper limit on the BF of $\mathcal{B}(B_s^0 \rightarrow \eta\eta') < 6.5 \times 10^{-5}$ [6].

4. $B_s^0 \rightarrow D_s^- X$

The inclusive decay $B_s^0 \rightarrow D_s^- X$ is an important decay as it provides information on f_s . This quantity gives the fraction of $b\bar{b}$ quarks that hadronize as B_s^0 mesons.

We study this mode using a semileptonic tagging method whereby we partially reconstruct the tag decay $B_s^0 \rightarrow D_s^- X \ell^+ \nu$, with $\ell = e, \mu$. The signal-side D_s^- is reconstructed from the remaining tracks in the event. This method is shown in Fig. 3. The decay channels of the D_s^- in the tag and signal decay channels are given in Table 1.

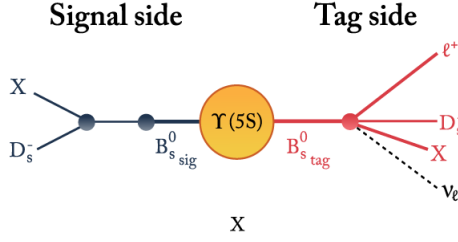


Figure 3: The semileptonic tagging method.

Tag Channel	Signal Channel
$\phi\pi^-$	$\phi(\rightarrow K^+K^-)\pi^-$
	$K_S^0(\rightarrow \pi^+\pi^-)K^-$
	$K^{*0}(\rightarrow K^\pm\pi^\mp)K^-$
$K_S^0K^-$	$\phi(\rightarrow K^+K^-)\pi^-$
	$K_S^0(\rightarrow \pi^+\pi^-)K^-$
	$K^{*0}(\rightarrow K^\pm\pi^\mp)K^-$

Table 1: D_s^- decay channels for the tag and signal channels.

The number of B_s^0 tags is obtained by performing a 2-dimensional binned maximum likelihood fit to the missing mass squared, M_{miss}^2 , and the D_s^- mass, $M(D_s^-)$, distributions for the yields for three categories. These three categories are correct tags; incorrect tags where the tag-lepton is combined with the signal-side D_s^- ; and other incorrect tags.

The number of signal-side D_s^- is obtained by performing a 3-dimensional binned maximum likelihood fit to the M_{miss}^2 and the signal- and tag-side invariant mass distributions.

Using Belle's full 121.4 fb^{-1} $\Upsilon(5S)$ data sample, we determine the BF $\mathcal{B}(B_s^0 \rightarrow D_s^- X) = [61.6 \pm 5.3 \text{ (stat.)} \pm 2.1 \text{ (syst.)}] \%$ and $f_s = 0.278 \pm 0.028 \text{ (stat.)} \pm 0.035 \text{ (syst.)}$ [7]. Our current BF result is smaller than the world average by approximately 1.2σ and smaller than the theoretical prediction of $86_{-13}^{+8} \%$. This may be explained by a higher than expected rate of excited $c\bar{s}$ states that decay to D (such as the $D_{s1}(2536)^\pm$) as opposed to D_s [7].

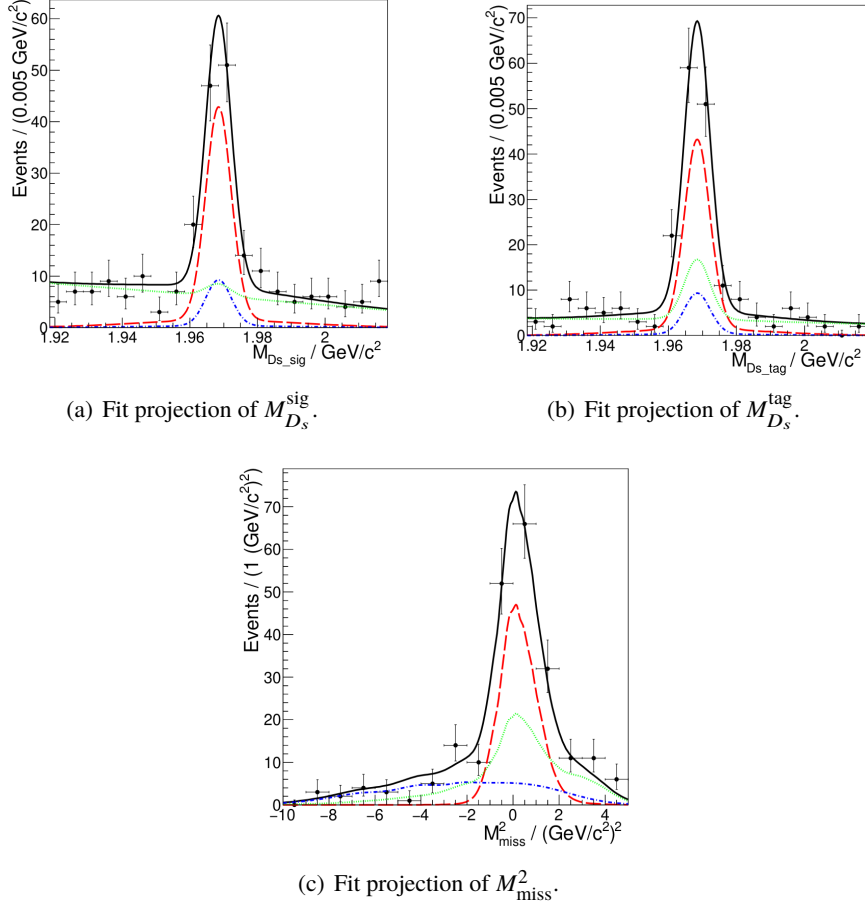


Figure 4: 1-dimensional fit projections of the 3-dimensional fit to the M_{miss}^2 and the signal- and tag-side invariant mass distributions. The data are the black points with errors bars, the signal is the red-dashed curve, the cross-feed is the blue dash-dotted curve, the background is the green dotted curve, and the sum is the solid black line. For each projection, the signal requirements of the other two are: $M_{\text{miss}}^2 \in [-2, 2] (\text{GeV}/c^2)^2$ and $M_{D_s}^{\text{sig}}$ and $M_{D_s}^{\text{tag}}$ are required to be in the range $M_{D_s}^{\text{PDG}} \pm 0.02 \text{ GeV}/c^2$ [7].

5. $B^+ \rightarrow K^+ K^- \pi^+$

The decay $B^+ \rightarrow K^+ K^- \pi^+$ is highly suppressed in the SM and is sensitive to new physics through BF enhancements. For this decay, LHCb has measured $\mathcal{A}_{CP} = -0.123 \pm 0.017 \pm 0.012 \pm 0.007$ and for the $M(K^+ K^-)$ range $1.0 < M(K^+ K^-) < 1.5 \text{ GeV}/c^2$, $\mathcal{A}_{CP} = -0.328 \pm 0.028 \pm 0.029 \pm 0.007$ [8–10].

Here we present our preliminary results. After the selections for background suppression are applied, we extract the signal by performing a 2-dimensional unbinned maximum likelihood fit in M_{bc} and ΔE , in bins of $M(K^+ K^-)$ and $M(K^+ \pi^-)$. Only the results from fitting in bins of $M(K^+ K^-)$ are used for \mathcal{A}_{CP} determination. Results from data and expectations from phase space (PHSP) Monte Carlo (MC), for the differential BF and \mathcal{A}_{CP} in bins of $M(K^+ K^-)$, are shown in Fig. 5¹. We obtain a weighted average, $\mathcal{A}_{CP} = -0.170 \pm 0.073(\text{stat.}) \pm 0.017(\text{syst.})$, over the whole

¹The $M(K^+ K^-)$ lower bound has been updated to $0.98 \text{ GeV}/c^2$, from $0.8 \text{ GeV}/c^2$ in Ref. [11].

$M(K^+K^-)$ range [11, 12]. There is a large \mathcal{A}_{CP} for $M(K^+K^-) < 1.1 \text{ GeV}/c^2$, which is found to be $-0.90 \pm 0.17(\text{stat.}) \pm 0.03(\text{syst.})$, at 4.8σ significance. The differential BF in bins of $M(K^+\pi^-)$ is shown in Fig. 6. We obtain a BF of $\mathcal{B}(B^+ \rightarrow K^+K^-\pi^+) = [5.38 \pm 0.40(\text{stat.}) \pm 0.35(\text{syst.})] \times 10^{-6}$.

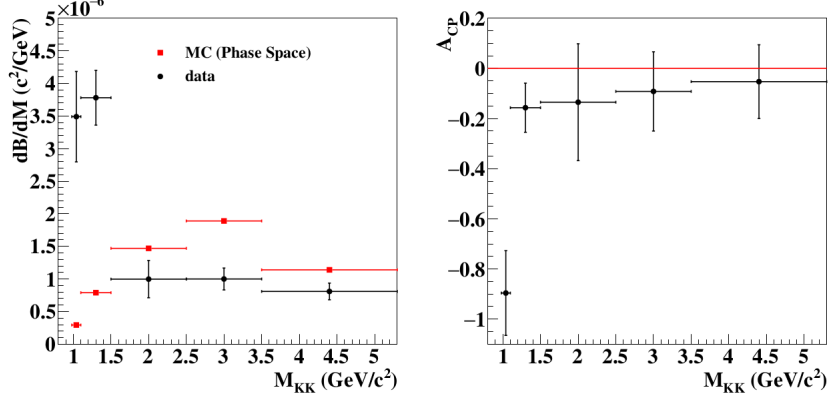


Figure 5: Differential BF (left) and measured \mathcal{A}_{CP} (right) results as a function of $M(K^+K^-)$. Black points are from data and red squared with error bars in the left figure are the signal expectations from a three-body PHSP MC sample that is rescaled to the experimental signal yield. Each point is obtained from the 2D fit with systematic uncertainties included [11, 12].

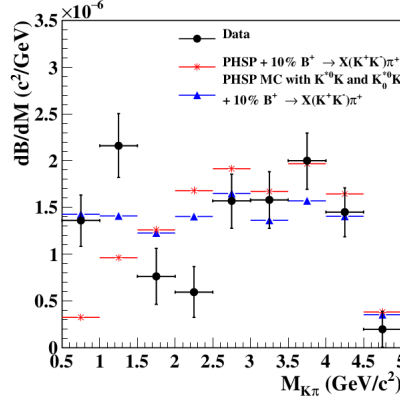


Figure 6: Differential BF results as a function of $M(K^+\pi^-)$. Black points are from data; red asterisks are expectations from a three-body PHSP MC sample with a 10% contribution from $B^+ \rightarrow X_{K^+K^-}\pi^+$ decays with spin-0; and the blue triangles show the results from the PHSP MC of adding the contribution from the intermediate states $B^+ \rightarrow K^{*0}K^+$ and $B^+ \rightarrow K_0^{*0}K^+$. All MC expectations are rescaled to the observed signal yield from the experimental data. Each point is obtained from the 2D fit with systematic uncertainties included [11, 12].

We also perform an angular analysis and present its results. We investigate the spin configuration of the K^+K^- system for $M(K^+K^-) < 1.1 \text{ GeV}/c^2$. Several MC samples of $B^+ \rightarrow X_{K^+K^-}(\rightarrow K^+K^-)\pi^+$, with different assumptions of the X spin state, are studied. In data we treat the $3.1 B^-$ signal events as background and subtract it from the $56.7 B^+$ signal events. We fit these events to different assumptions of the spin model: spin-0, spin-1, spin-2, and a coherent sum model given in equation 1, which models the coherent sum of the S - and P -wave contributions.

$$f(\cos(\theta_{\text{hel}})) = A_S^2 + 2A_S A_P \cos(\theta_{SP}) P_1(\cos(\theta_{\text{hel}})) + A_P^2 P_1^2(\cos(\theta_{\text{hel}})) \quad (1)$$

Here the helicity angle, θ_{hel} , is defined as the angle between the momenta of the B meson and the same-charge kaon (both are evaluated in the X rest frame); P_1 is the first-order Legendre polynomial; $\cos(\theta_{SP})$ is the relative phase; and A_S and A_P are the S - and P -wave amplitudes, respectively.

We find that the data is not well described by pure S -, P -, or D -wave models and favors the coherent sum model. After performing the fit, the amplitudes $A_S = 4.6 \pm 2.0$ and $A_P = 9.2 \pm 2.8$ are obtained. This is consistent with a large P -wave contribution [12].

6. Summary and Conclusion

Searches for four hadronic B/B_s^0 decays have been presented. The searches for the decays $B_s^0 \rightarrow \eta' X_{s\bar{s}}$ and $B_s^0 \rightarrow \eta\eta'$ are the world's first. They are probes of new physics and may help in understanding the η' mass. The measurement of $B_s^0 \rightarrow D_s^- X$ provides information on the rate of $b\bar{b}$ hadronization to B_s^0 mesons.

The measurement of $B^+ \rightarrow K^+ K^- \pi^+$ confirms LHCb's result of a large \mathcal{A}_{CP} in the low $M(K^+ K^-)$ range and we report a coherent-sum spin structure for the $K^+ K^-$ system.

References

- [1] BELLE COLLABORATION *Phys. Rev. D* **87** (2013) 031101.
- [2] BELLE COLLABORATION *Phys. Rev. D* **104** (2021) 012007.
- [3] UNIVERSITY OF MISSISSIPPI, A. Datta, private communication.
- [4] BABAR COLLABORATION *Phys. Rev. Lett.* **93** (2004) 061801.
- [5] T. Sjöstrand, S. Mrenna and P. Skands *J. High Energy Physics* **2006** (2006) 026–026.
- [6] BELLE COLLABORATION *Phys. Rev. D* **104** (2021) L031101.
- [7] B. Wang et al., 2021 [hep-ex:2106.11265], Submitted to *Phys. Rev. D*.
- [8] LHCb COLLABORATION *Phys. Rev. Lett.* **112** (2014) 011801.
- [9] LHCb COLLABORATION *Phys. Rev. D* **90** (2014) 112004.
- [10] LHCb COLLABORATION *Phys. Rev. Lett.* **123** (2019) 231802.
- [11] BELLE COLLABORATION *Phys. Rev. D* **96** (2017) 031101.
- [12] C.-L. Hsu et al., Paper in preparation for *Phys. Rev. D*.